Design of EBG Power Distribution Networks With VHF-Band Cutoff Frequency and Small Unit Cell Size for Mixed-Signal Systems

Ki Hyuk Kim, *Member, IEEE*, and José E. Schutt-Ainé, *Fellow, IEEE*

***Abstract*—Hybrid electromagnetic bandgap (EBG) power distribution networks (PDNs) with VHF-band cutoff frequency, small unit cell size, and wideband noise suppression characteristics are proposed. Commercial lumped chip inductors are used to implement inductive bridges between neighboring metal patches instead of conventional microstrip lines. A 1-D analysis model of the EBG structure is developed to find a mathematical ground for the use of the lumped chip inductors in the EBG PDN designs. From 158 MHz to 4528 MHz a measured stopband bandwidth of 4.37 GHz is achieved with over −60 dB noise suppression levels.**

***Index Terms*—Electromagnetic bandgap (EBG), power distribution network (PDN), simultaneous switching noise (SSN).**

I. Introduction

As CLOCK frequencies of digital circuits rapidly increase, simultaneous switching noise (SSN) degrades not only the noise margins of digital circuits, but also the performance of analog circuits in the case of mixed-signal systems. In order to minimize the switching noise coupling, several noise suppression methods have been proposed such as gapped- or island-type power plane structures [1], a resistive termination method [2], and efficient bypassing techniques, e.g., shorting vias and capacitive walls [3]. Recently, a power distribution network (PDN) using a uniplanar electromagnetic bandgap (EBG) structure was proposed by Wu *et al.* [4]. The uniplanar EBG structures are easily designed and fabricated using standard printed circuit board (PCB) technology, since specially designed vias and additional inter-plane metal patches that are the basic building blocks of mushroom-type EBG structures [5] are not required.

A unit cell of the uniplanar EBG structure consists of two neighboring metal patches and a bridge; as a result, a 1-D or 2-D array of the unit cells has bandstop filter characteristics due to shunt capacitances of the patches and series inductances and capacitances of the bridges. However, because of the low inductance of the bridges which are implemented using microstrip lines, the cutoff frequency of Wu's structure is around 1 GHz. To increase the inductance of the microstrip line bridges, several EBG structures are proposed [6]–[8]. Basically, the inductance values of the published bridges are increased by extending the lengths of the microstrip lines at the expense of the uniformity of the metal patches. However, these sacrifices not only reduce the power capacity of the EBG PDNs, but also increase the signal integrity (SI) problems of high speed signal lines over the perforated uniplanar EBG planes. Moreover, the lowest cutoff frequency [7] of the previous EBG PDNs is still higher than the clock frequencies of current mixed-signal systems [9] and their physical sizes are not applicable to small form factor structures.

In this letter, EBG PDNs with VHF-band cutoff frequencies and small unit cell size characteristics are proposed. Commercially available high inductance lumped chip inductors are used as the bridges, in spite of their low self resonant frequencies (SRFs). A 1-D analysis model of the EBG structure is developed. And it is shown that the parasitic series capacitance and the intrinsic inductance of the bridges are independent with the cutoff frequency and high frequency characteristics of the EBG structure, respectively. The lowpass cutoff frequency of the EBG structure is only dependent on the capacitances of the square metal patches and the inductances of the bridges. Based on the analysis results, an EBG PDN with small unit cell size and VHF-band cutoff frequency is designed for mixed-signal system applications.

II. One-Dimensional Analysis of EBG Structure

A. Equivalent Circuit Modeling of Uniplanar EBG Structure

Fig. 1 shows an equivalent LC model of the 1-D periodic uniplanar EBG structure. Components within the dotted rectangle correspond to the ith unit cell of the structure, where a and g are the center-to-center distance and the gap size between two neighboring patches, respectively, b is the width of the patches, and d is the height of the dielectric substrate. L_P and C_P are the inductance and the capacitance of each square metal patch, respectively, $C_{\rm gap}$ is the gap capacitance, and L_L and $C_{\rm parasitics}$ are the inductance and the parasitic series capacitance of the bridge, respectively. C_T is a summation of $C_{\rm gap}$ and $C_{\rm parasitics}$, and L_P, C_P, and $C_{\rm gap}$ can be calculated using the following equations [10]:

$$L_P = \mu_0 d \tag{1}$$

$$C_P = \varepsilon_r \varepsilon_0 \frac{b^2}{d} \tag{2}$$

$$C_{\rm gap} = b\frac{\varepsilon_0 (1+\varepsilon_r)}{\pi} \cdot \cosh^{-1}\left(\frac{a}{g}\right). \tag{3}$$

Manuscript received January 12, 2007; revised March 15, 2007. This work was supported by the IT Scholarship Program Supervised by the Institute for Information Technology Advancement (IITA) and by the Ministry of Information and Communication (MIC), Korea.

The authors are with the Department of Electrical and Computer Engineering, University of Illinois, Urbana, IL 61801 USA (e-mail: khkim@emlab.uiuc.edu; jschutt@emlab.uiuc.edu).

Color versions of one or more of the figures in this letter are available online at http://ieeexplore.ieee.org.

Digital Object Identifier 10.1109/LMWC.2007.899299

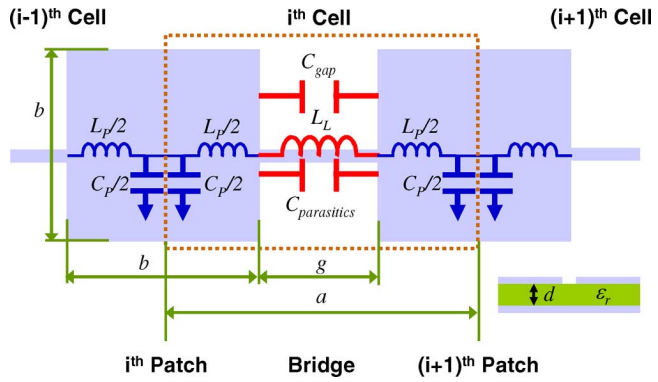

Fig. 1. One-dimensional equivalent circuits of EBG PDN.

In the above equations, ε_0 and μ_0 are the free-space permittivity and permeability, respectively, and ε_r is the relative permittivity of the dielectric material. It is important to note that the capacitance ratios C_{gap}/C_P and $C_{\text{parasitics}}/C_P$ are very small for typical PCB/package structures where the widths of patches are much larger than the heights of PCB/package. $C_{\text{parasitics}}$ varies depending on physical implementations of the bridges, e.g., microstip line, stripline, bondwire, and chip inductor. When the bridges are implemented using lumped chip inductors, typical parasitic capacitance values ($C_{\text{parasitics}}$) range from 0.09 to 0.24 pF for inductance values in the 47–560 nH range [11], which is smaller than C_{gap} under the condition that $b \cdot (1 + \varepsilon_r)$ is larger than $C_{\text{parasitics}} \cdot (118.6e + 12)$ mm for EBG structures with $g = 0.1 \cdot a$. This relationship is obtained by equating $C_{\text{parasitics}}$ to the right-hand side of (3). For the 47–560 nH inductance range, the calculated values of $C_{\text{parasitics}} \cdot (118.6e + 12)$ is only 8.5%–22.6% of the calculated values of $b \cdot (1 + \varepsilon_r)$ using parameters of the previously published EBG structures [4], [6]–[8].

B. Stopband Cutoff Frequencies of 1-D EBG PDN

The image parameter method [10] and previous two capacitance ratios are used to analyze the 1-D EBG structure. The derived lower (f_{lower}) and upper (f_{upper}) cutoff frequencies of the EBG structure are

$$f_{\text{lower}} = \left[\pi\sqrt{C_P\,(L_P + L_L)}\right]^{-1} \tag{4}$$

$$f_{\text{upper}} = \left[2\pi\sqrt{\frac{C_T C_P L_P}{(4C_T + C_P)}}\right]^{-1}. \tag{5}$$

f_{lower} has no dependency on C_T, and this enables the use of high inductance lumped chip inductors as the bridges, although they have low SRFs due to the parasitic series capacitances. In addition, there is no bandwidth degradation due to the increased inductance, because the bridge inductance is independent of f_{upper}. However, f_{upper} is typically higher than the first resonant frequency of the metal patches ($= 1/(2 \cdot \sqrt{L_P C_P})$). In that case, the value of f_{upper} is useless, and the rectangular cavity resonant frequencies of the patches become dominant.

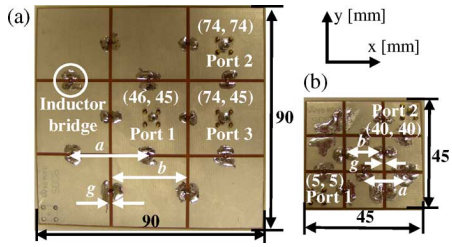

Fig. 2. Fabricated EBG PDNs: (a) TV-A and (b) TV-B.

TABLE I
DETAILS OF DESIGN PARAMETERS FOR THE PROPOSED EBG PDNS

Type of EBG	a [mm]	b [mm]	g [mm]	Array of Patches	L_L [nH]/ $C_{parasitics}$ [pF]
TV-A	30	28.7	1.3	3×3	560/ 0.16
TV-B	15	13.7			

III. Design and Experimental Verification of Proposed Hybrid EBG PDNs

Fig. 2(a) and (b) show the fabricated EBG PDNs with 90×90 mm^2 (test vehicle A: TV-A) and 45×45 mm^2 (test vehicle B: TV-B) areas, respectively. The thickness and the dielectric constant of the FR-4 substrate are 0.4 mm and 4.4, respectively. Details of the design parameters are summarized in Table I, and locations of all ports are shown in Fig. 2. In the case of the TV-A, the physical dimensions and port locations are the same as those of [6] in order to directly compare the noise suppression performances. Only the microstrip line bridges are replaced by the lumped chip inductors, and Coilcraft, Inc., 0603-LS-561 560 nH chip inductors [11] are used in this work. The TV-B which occupies only 25% area of the TV-A is designed for small form factor PCBs and packages.

Fig. 3(a) and (b) show the measured insertion loss characteristics of the TV-A and -B, respectively. Agilent E8358A PNA Series Network Analyzer was used to measure the S parameters of the TV-A and -B at the 300 kHz to 9 GHz frequency range. For brevity only $|S21|$ responses are plotted. The open circles and solid rectangles represent the measured $|S21|$ of the PDNs without and with the proposed EBG structure, respectively. The cross symbols in Fig. 3(a) represent the simulated $|S21|$ responses of reference EBG PDN [6] using Ansoft HFSS. The calculated and measured lower cutoff frequencies and measured -60 dB noise suppression bandwidths of each test vehicle are summarized in Table II. An approximate 750 MHz cutoff frequency enhancement is achieved and the enhancement can be further increased by using higher inductance values for the chip inductors. The low frequency resonant peak of the reference EBG PDN [6] is caused by the microstrip line bridges, and can be suppressed by adding series resistors [12]. However, this is not an optimal solution to the PDN designs. Our proposed EBG PDNs effectively remove the resonance by lowering the lower cutoff frequency. The lower cutoff frequency is defined as a frequency where the $|S21|$ responses start to decrease monotonically. Although the bridge inductance of TV-A is equal to that of TV-B, the f_{lower} of TV-B is 2.1 times higher than that of TV-A, because the patch area is 4.4 times smaller. However, the

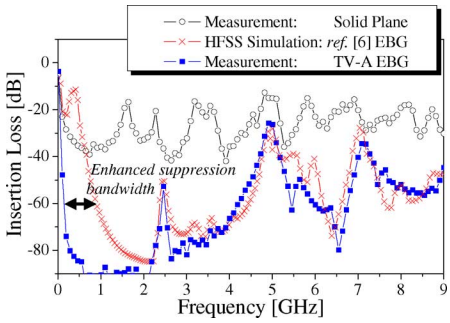

(a)

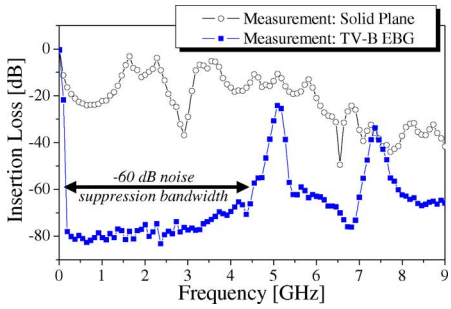

(b)

Fig. 3. (a) $|S21|$ responses of TV-A EBG PDN. 3 and (b). $|S21|$ responses of TV-B EBG PDN.

TABLE II
SUMMARY OF NOISE SUPPRESSION CHARACTERISTICS OF EBG PDNS

Types of EBG	Parameters	1-Dimensional Analysis	S-parameter Measurement
[6]	-60 dB Suppression [MHz]	N.A.	900 – 2370 and 2550 – 4440
TV-A			158 – 2419 and 2515 – 4354
TV-B			158 – 4528
TV-A	f_{lower}/f_{upper} [MHz]	47.5/ 5482	47.2/ N.A.
TV-B		99.4/ 8558	106.1/ N.A.

increased number of unit cells within the same port distances makes the $|S21|$ slope of TV-B steeper than that of TV-A. It is important to note that there is almost no degradation of high frequency characteristics, and the noise suppression bandwidths are enhanced due to the reduction of the cutoff frequencies.

Several peaks of the insertion loss responses are due to the cavity resonance modes of the patches, e.g., peaks at 2.48, 4.95, and 7.11 GHz in Fig. 3(a) are corresponding to the (1, 0), (2, 0), and (2, 2) resonant modes of 28.7×28.7 mm^2 metal patches, and peaks at 5.14 and 7.36 GHz in Fig. 3(b) are corresponding to the (1, 0) and (1, 1) resonant modes of 13.7×13.7 mm^2 metal patches. These resonant frequencies cannot be predicted, since the high frequency distributed effects of the patches are not considered in the 1-D analysis model of the patches.

IV. CONCLUSION

In this letter, a 1-D analysis model of the EBG structure is developed to give the background for the use of lumped chip inductors as the bridges in EBG PDN designs. Based on analysis results, a hybrid EBG structure with VHF-band cutoff frequency and small unit cell size characteristics is proposed. Wideband noise suppression characteristics are also achieved using proposed hybrid EBG PDNs.

REFERENCES

[1] W. Cui, J. Fan, Y. Ren, H. Shi, J. L. Drewniak, and R. E. DuBroff, "DC power-bus noise isolation with power-plane segmentation," *IEEE Trans. Electromagn. Compat.*, vol. 45, no. 2, pp. 436–443, May 2003.

[2] I. Novak, "Reducing simultaneous switching noise and EMI on ground/power planes by dissipative edge termination," *IEEE Trans. Adv. Packag.*, vol. 22, no. 3, pp. 274–283, Aug. 1999.

[3] T. Tarvainen, "Simplified modeling of parallel plate resonances on multilayer printed circuit boards," *IEEE Trans. Electromagn. Compat.*, vol. 42, no. 3, pp. 284–289, Aug. 2000.

[4] T.-L. Wu, Y.-H. Lin, and S.-T. Chen, "A novel power planes with low radiation and broadband suppression of ground bounce noise using photonic bandgap structures," *IEEE Microw. Wireless Compon. Lett.*, vol. 14, no. 7, pp. 337–339, Jul. 2004.

[5] T. Kamgaing and O. M. Ramahi, "A novel power plane with integrated simultaneous switching noise mitigation capability using high impedance surface," *IEEE Microw. Wireless Compon. Lett.*, vol. 13, no. 1, pp. 21–23, Jan. 2003.

[6] T.-L. Wu, C.-C. Wang, Y.-H. Lin, T.-K. Wang, and G. Chang, "A novel power plane with super-wideband elimination of ground bounce noise on high speed circuits," *IEEE Microw. Wireless Compon. Lett.*, vol. 15, no. 3, pp. 174–176, Mar. 2005.

[7] X.-H. Wang, B.-Z. Wang, Y.-H. Bi, and W. Shao, "A novel uniplanar compact photonic bandgap power plane with ultra-broadband suppression of ground bounce noise," *IEEE Microw. Wireless Compon. Lett.*, vol. 16, no. 5, pp. 267–268, May 2006.

[8] J. Qin and O. M. Ramahi, "Ultra-wideband mitigation of simultaneous switching noise using novel planar electromagnetic bandgap structures," *IEEE Microw. Wireless Compon. Lett.*, vol. 16, no. 9, pp. 487–489, Sep. 2006.

[9] Analog Devices, Inc., "ADC Selection Matrix," Tech. Rep., 2007 [Online]. Available: http://www.analog.com

[10] J. Choi, "Noise Suppression and Isolation in Mixed-Signal Systems Using Alternating Impedance Electromagnetic Bandgap (AI-EBG) Structure," Ph.D. dissertation, School Elect. Comput. Eng., Georgia Inst. Technol., Atlanta, 2005.

[11] Coil Craft, Inc., "Datasheets," Tech. Rep., 2007 [Online]. Available: http://www.coilcraft.com

[12] M. Hampe and S. Dickmann, "Improving the behavior of PCB power-bus structures by an appropriate segmentation," in *Proc. IEEE Int. Symp. Electromagn. Compat.*, 2005, pp. 961–966.